DOI: 10.1002/chem.200501189

Comparative Analyses of a Family of Potential Self-Replicators: The Subtle Interplay between Molecular Structure and the Efficacy of Self-Replication

Russell J. Pearson, Eleftherios Kassianidis, Alexandra M. Z. Slawin, and Douglas Philp*[a]

Abstract: It is envisioned that protocols based on self-replication will emerge as a formidable synthetic apparatus for the production of nanoscale assemblies through molecular structures that are capable of automultiplication with high reaction rates and selectivities. To achieve this goal, a complete understanding of the relationship between molecular structure and replication efficiency is necessary. Rigorous experimental and theoretical analyses of a series of self-complementary scaffolds that are intimately related in a constitutional sense, manufactured through the Diels–Alder reaction of complementary subunits, were undertaken. Experimental and computational methods were employed to map the key determinants that dictate the emergence of self-replicative function, as well as the efficiency, rate and selectivity of the self-replicative processes.

Keywords: kinetics · molecular recognition · recognition-mediated reactions · self-replication · supramolecular chemistry

Introduction

The Diels–Alder reaction is encountered frequently in the syntheses of natural products. However, only a limited number of naturally occurring *Diels–Alderases* have, so far, been identified[1] and characterised. From a purely chemical perspective, this reaction is an ideal means of introducing six-membered rings in a simple one-step process under mild conditions. Some Diels–Alder reactions[2] can, however, be either extremely slow, requiring a month or more to achieve only moderate yields, or rather unselective in either a stereochemical or regiochemical sense. As a consequence, many methods of accelerating the rate of these cycloadditions have been employed over the years. The use of high pressure,[3] ionic liquids,[4] altering solvent polarity,[5] or the use of a suitable Lewis acid catalyst,[6] have all been described as a means of achieving this goal.

Although structural information on natural *Diels–Alderases*[7] is sketchy, it is very likely that they employ noncovalent interactions, such as aromatic stacking, electrostatic interactions, hydrogen bonding and van der Waals contacts, as effective tools to ensure that the reactive centres are held in the correct orientation for the preferred reaction to occur. Synthetic hosts[8] and catalytic antibodies[9] that are capable of accelerating Diels–Alder cycloadditions have been described. We are interested in accelerating and introducing selectivity to chemical reactions through the framework[10] of the autocatalytic self-replicating system shown in Figure 1.

Self-template **T** is initially produced through the covalent union of its constituent fragments **A** and **B** (distinguished by steric, geometrical and recognition[11] surface complementarity) in an uncatalysed bimolecular fashion (designated by rate constant k_{bim}: Channel 1 in Figure 1).

In the initial phases of the process, high levels of the binary[12] complex [**A**·**B**] are formed (favoured entropically as it requires only a singe recognition event, denoted by equilibrium constant K_{ass}: Channel 2 in Figure 1). Within complex [**A**·**B**], the juxtaposition of the reactive centers of **A** and **B** is attainable, rendering the reaction[13] between **A** and **B** pseudounimolecular. Intracomplex reactions of this sort are characterised by rate accelerations[14] of considerable magnitude, relative to the rate of random bimolecular collisions between **A** and **B**, and yield $\mathbf{T}_{inactive}$ with a rate constant of k_{AB} ($k_{AB} \gg k_{bim}$). $\mathbf{T}_{inactive}$ is a conformer of **T** in which the recognition sites are associated intramolecularly, and is, therefore, devoid of any intermolecular recognition

[a] Dr. R. J. Pearson, Dr. E. Kassianidis, Prof. A. M. Z. Slawin, Dr. D. Philp
Centre for Biomolecular Sciences
School of Chemistry, University of St Andrews
North Haugh, St Andrews KY16 9ST (UK)
Fax: (+44) 1334-463-808
E-mail: d.philp@st-andrews.ac.uk

Supporting information for this article is available on the WWW under http://www.chemeurj.org/ or from the author.

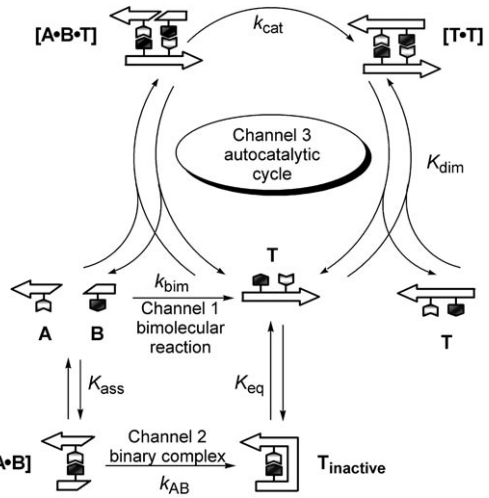

Figure 1. Minimal model of self-replication. Reagents **A** and **B** can react in three ways. Channel 1: uncatalysed bimolecular reaction; Channel 2: recognition-mediated pseudounimolecular pathway mediated by binary complex [**A**·**B**]; Channel 3: recognition-mediated pseudounimolecular autocatalytic cycle mediated by ternary complex [**A**·**B**·**T**].

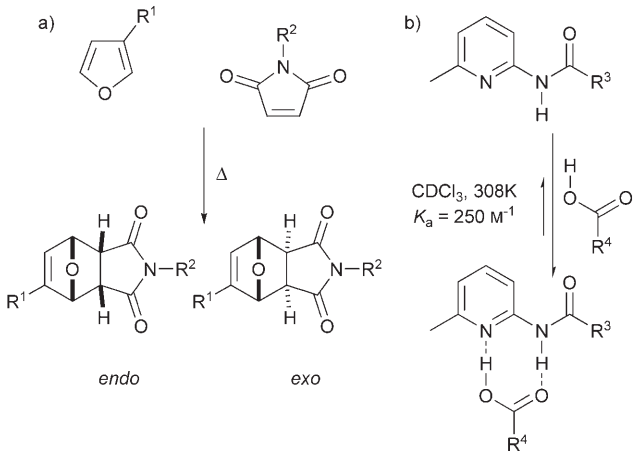

Scheme 1.

capabilities. The ability of $\mathbf{T}_{\mathbf{inactive}}$ to interconvert to **T** (K_{eq}) is dependent upon the geometrical features and rigidity present in the molecular structure. Clearly, in certain circumstances the equilibrium for this interconversion will lie far in favour of $\mathbf{T}_{\mathbf{inactive}}$ and self-replication is eradicated.

If reaction through Channel 2 is not possible for steric or electronic reasons, the concurrent preorganisation of **A** and **B** on the peripheral recognition domains of **T** results in the formation of catalytic ternary complex [**A**·**B**·**T**], signifying initiation of the autocatalytic[15] cycle. Optimum alignment and approximation of reactive functionalities of **A** and **B** within [**A**·**B**·**T**] leads to production of cyclic antiparallel dimer [**T**·**T**] at an accelerated rate (expressed as k_{cat}, for which $k_{cat} > k_{bim}$: Channel 3 in Figure 1). Disassembly of [**T**·**T**] (K_{dim}) extricates the offspring from the parent template, and both the parent template and its newly formed offspring enter new autocatalytic cycles. Because the number of template molecules is doubled with each cycle reiteration, an exponential[16] concentration–time profile is anticipated for **T**.

Results and Discussion

Intrigued by the problematic, and often intractable, behaviour[17] of organic self-replicating systems, we endeavoured to establish clear relationships between the relative orientations of the reactive and recognition sites in a particular system and its kinetic behaviour. Accordingly, systematic analyses (kinetic and computational) of a small library of eight structurally related putative self-replicators were undertaken. The Diels–Alder reaction between furan and maleimides (Scheme 1a) was chosen as the means of forming covalent bonds in the recognition-mediated systems because its mechanism is well understood and the reaction possesses[18,19] strict stereoelectronic demands. The association between amidopicolines and carboxylic acids (Scheme 1b) was chosen as the means of noncovalently associating the constituent building blocks of our replicating systems.

By applying the principles of skeletal simplicity and bifunctionality, prosthetic, mutually complementary recognition elements were appended to the reactive sites of precursor dienes and dienophiles, respectively, by means of aliphatic tethers. Methylene or bismethylene chains were utilised to connect 2-amidopicoline functionalities to the 3-position of the furan dienes (compounds **1** and **2**) and carboxylic acid functionalities to the maleimide rings of dienophiles (compounds **3b** and **4b**).

Intermolecular recognition within Systems 1–4 (Scheme 2) was directed by formation of parallel hydrogen-bond diads[20] between amidopicoline and carboxylic acid moieties. The amidopicoline moiety constitutes a sterically accessible hydrogen-bonding microenvironment to which the carboxylic acid moiety is electronically complementary.

In the achiral environments (substrates, media), in which kinetic investigations were undertaken, the enantiotopic faces of dienes **1** and **2** remain undifferentiated, thereby precluding any prospects of stereoinduction to the product(s). Additionally, utilisation of symmetrical dienophiles **3** and **4** automatically eradicated any regioselectivity issues. Under such conditions, the furans engage their complementary counterparts, the maleimides, in pericyclic[21] unions via intermediacy of two transition states, *endo* and *exo*, on the basis of relative orientations of the furan and maleimide nuclei in the pretransition-state phase. This furnishes pairs of racemic, diastereoisomeric adducts *endo* and *exo* (Scheme 2), distinguished by the spacers connecting the hydrogen-bonding sites to the cycloadduct core.

For each system, we wished to establish the dominant recognition-mediated pathway (Figure 1) for reaction of the diene with the dienophile. Note that either diene **1** or **2** in combination with dienophile **3b** or **4b** (Scheme 2) can be considered equivalent to building blocks **A** and **B** in

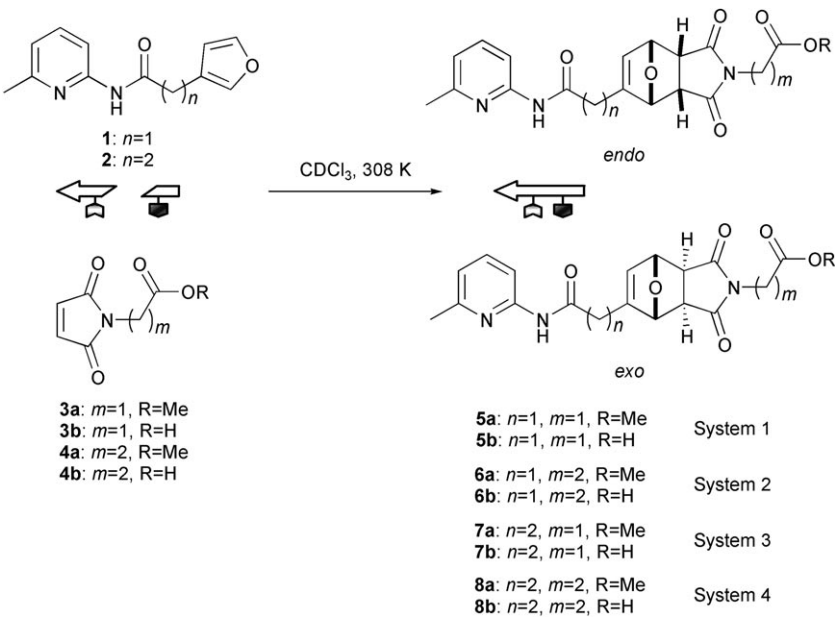

Scheme 2.

Figure 1. To accomplish this task, we first measured the rates of the recognition-mediated reactions between pairwise combinations of furans **1** and **2** and maleimides **3b** and **4b** by using 500 MHz ^{1}H NMR spectroscopy in $CDCl_3$ at 308 K. In all cases, the starting concentration of each reagent was 25 mM.

Further experiments were required to establish which recognition-mediated reaction channel was dominant in each system. The intrinsic rate and diastereoselectivity of the nonrecognition-mediated bimolecular cycloaddition reaction was determined by pairwise combination of furans **1** and **2** with the appropriate maleimide esters **3a** and **4a** under identical reaction conditions. The precise nature of the recognition-mediated processes present in each system (Channel 2 versus Channel 3, Figure 1) was determined through additional kinetic experiments.

Recognition-mediated reactivity could be demonstrated by the addition of a competitive inhibitor to the reaction mixture. In these experiments, diene **1** or **2** was mixed with dienophile **3b** or **4b** and a competitive inhibitor of the amido–picoline recognition motif was added in the form of four equivalents of benzoic acid. A reduction in the rate and/or diastereoselectivity of the reaction in the presence of benzoic acid indicates that a recognition-mediated process is operating in the system. Given the presence of a ternary complex in the autocatalytic cycle (Channel 3, Figure 1), a template-directed process would be affected to a greater degree by a hydrogen-bond competitor than by a reactive binary complex (Channel 2, Figure 1).

If the reaction proceeds by a replicating mechanism, that is, the reaction is template directed, the addition of substoichiometric amounts of template at the start of the reaction should increase its initial rate. The disappearance of a lag period in the reaction on addition of template provides direct evidence that the reaction is template directed, suggesting that self-replication (Channel 3, Figure 1) is present.

Ultimately, the manipulation of chemical reactivity by these subtle approaches allows a better appreciation of the structural sensitivity governing the dominant recognition-mediated reaction channel(s), shown in Figure 1.

System 1: The reaction of **1** with **3a** or **3b** to give *endo*-**5a** and *exo*-**5a** or *endo*-**5b** and *exo*-**5b**, respectively, provides the shortest possible tether-length combination for the series, with a single methylene spacer on each building block (System 1, Scheme 2). The kinetic data recorded for this system are shown in Figure 2. The introduction of recognition into this system doubles the overall product concentration after 14 h. Additionally, both *endo*-**5b** and *exo*-**5b** respond to the addition of preformed template, suggesting that both templates are capable of accelerating their own formation. These observations were reinforced by simulation and fitting of the experimental data[22] to a kinetic model in which *endo*-**5b** and *exo*-**5b** are formed through self-replication. Despite the enhancements in the overall rate of product formation, the diastereoselectivity of the reaction actually diminished; [*endo*-**5b**:*exo*-**5b**] dropped from 3:1 in the absence of recognition to 5:3 in the presence of recognition. This loss of diastereoselectivity is a direct result of the stronger recognition-mediated acceleration of the formation of *exo*-**5b**.

Molecular mechanics calculations reveal that the lowest-energy conformations of *exo*-**5b** all have an open geometry (Figure 3a), with the recognition sites available to associate with further molecules of **1** and **3b** to form the corresponding ternary complex [**1**·**3b**·*exo*-**5b**] and ultimately the *exo* homodimer. By contrast, the lowest-energy conformations of *endo*-**5b** adopt closed conformations (Figure 3b) suggestive of reaction through a binary reactive complex. The rates of formation of *exo*-**5b** and *endo*-**5b** both show a response to the addition of the appropriate template. This behaviour suggests that, in both cases, the catalytic ternary complexes [**1**·**3b**·*exo*-**5b**] and [**1**·**3b**·*endo*-**5b**] are active in a kinetic sense. To probe this hypothesis further, we examined the coconformations of the two product homodimers [*exo*-**5b**·*exo*-**5b**] and [*endo*-**5b**·*endo*-**5b**] and the putative heterodimer [*exo*-**5b**·*endo*-**5b**]. Both homodimers exhibit stable dimeric structures containing four hydrogen bonds; as an example, the structure of [*exo*-**5b**·*exo*-**5b**] is shown in Figure 3c. Be-

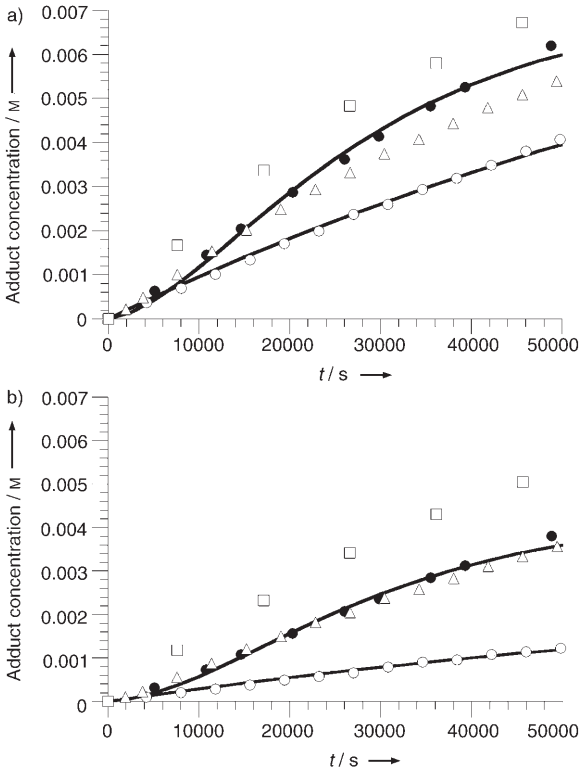

Figure 2. Rate profiles, at 308 K in $CDCl_3$, for formation of (a) *endo*-**5a** or *endo*-**5b** and (b) *exo*-**5a** or *exo*-**5b** from building blocks **1** and **3a**, and **1** and **3b**, respectively. Starting concentrations of diene and dienophile were 25 mM. ●: Reaction between **1** and **3b** (recognition-mediated reaction); ○: reaction between **1** and **3a** (bimolecular reaction); △: reaction between **1** and **3b** in the presence of 4 equiv of $PhCO_2H$ (competitive inhibitor); □: reaction between **1** and **3b** in the presence of preformed *endo*-**5b** (19 mol%) or *exo*-**5b** (13 mol%). Solid lines represent the best fit of experimental data to the appropriate kinetic model by using the SimFit[22] package. See Supporting Information for further details of the kinetic models used.

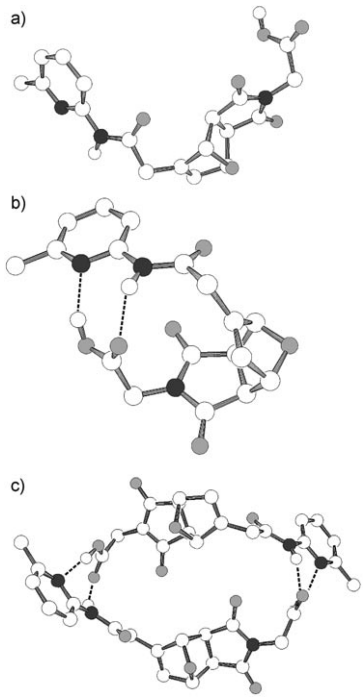

Figure 3. Ball-and-stick models of representative low-energy conformations of (a) *exo*-**5b**, (b) *endo*-**5b**, and (c) [*exo*-**5b**·*exo*-**5b**] calculated by using the AMBER* forcefield. Carbon atoms white, oxygen atoms light grey, nitrogen atoms dark grey. Some hydrogen atoms are omitted for clarity. Hydrogen bonds are represented by dashed lines.

cause the transition state in the cycloaddition reaction occurs relatively late, it is likely that the transition states leading to *exo*-**5b** and *endo*-**5b** are also reasonable fits to the respective templates. More interestingly, there is a fundamental incongruence between *exo*-**5b** and *endo*-**5b**; no low-energy structure of [*exo*-**5b**·*endo*-**5b**] contains more than two hydrogen bonds and, therefore, it seems unlikely that one diastereoisomeric template could support the transition state for the other. This result may indicate that antagonistic diastereospecific replication cycles, similar to those reported previously by our group[23], are operating in this system.

System 2: The introduction of an additional methylene unit into the dienophile component of the Diels–Alder reaction affords System 2 (Scheme 2). In contrast to System 1, the control reaction between **1** with **4a** is unselective and affords an equimolar mixture of *endo*-**6a** and *exo*-**6a** after 14 h. The introduction of recognition into this system results in 3:1 selectivity for *endo*-**6b** over *exo*-**6b** with a two-fold increase in reaction rate. The insolubilities of *endo*-**6b** and *exo*-**6b** prevented a complete analysis of the kinetic behaviour of this system because experiments involving added template could not be performed. However, molecular-modelling studies (Figure 4), suggest that the selectivity for *endo*-**6b** is derived from binary-complex reactivity. The lowest-energy conformations of *endo*-**6b** all exhibit a closed geometry with two hydrogen bonds. By contrast, all of the low-energy conformations of *exo*-**6b** exhibit open geometries. These observations suggest that the most likely recognition-mediated pathway for the formation of *endo*-**6b** is the binary-reactive-complex channel. Although *exo*-**6b** could potentially form a ternary complex with **1** and **4b**, the apparently low efficiency of the ternary complexes in System 1 and the presence of the extra methylene group in **4b** would make the [**1**·**4b**·*exo*-**6b**] ternary complex kinetically insignificant.

System 3: Placing a CH_2CH_2 spacer between the recognition site and the diene, and a single methylene between the recognition site and the dienophile, affords System 3 (Scheme 2). Reaction of furan **2** with maleimides **3a** and **3b** saw the rate and ratio of product formation change once again (Figure 5). In this system, the incorporation of recognition significantly improves the selectivity from 1.6:1 to 5:1 in favour of *endo*-**7b**. In addition, the rate of product formation is increased by almost three-fold. In contrast to System 1, the extra methylene unit in the furan building block in this system directs reaction through the reactive binary com-

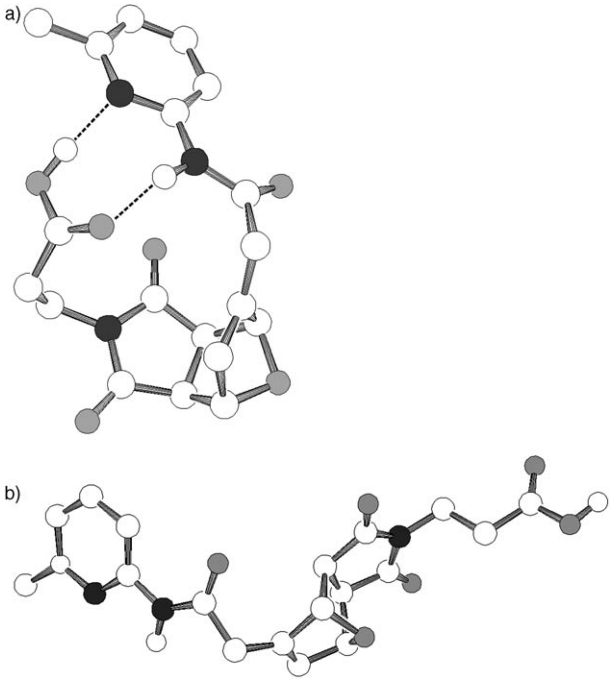

Figure 4. Ball-and-stick models of representative low-energy conformations of (a) *endo*-**6b** and (b) *exo*-**6b** calculated by using the AMBER* forcefield. Carbon atoms white, oxygen atoms light grey, nitrogen atoms dark grey. Some hydrogen atoms are omitted for clarity. Hydrogen bonds are represented by dashed lines.

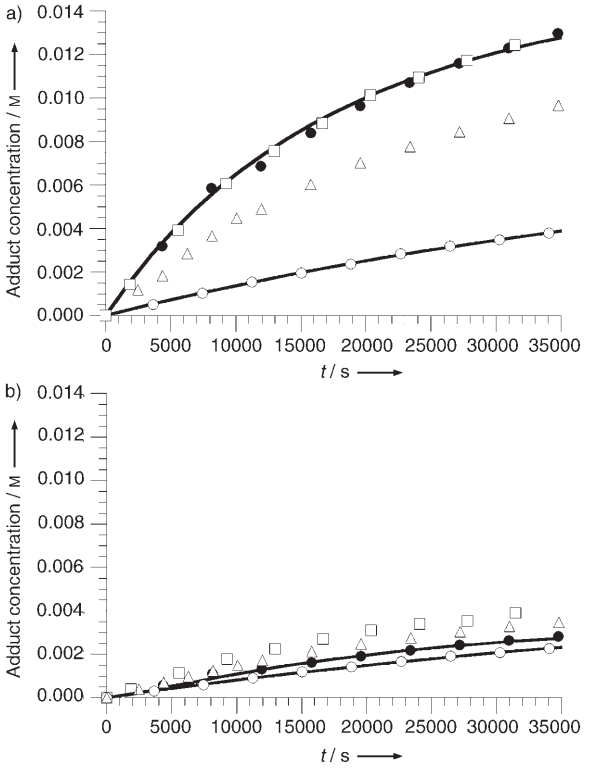

Figure 5. Rate profiles, at 308 K in $CDCl_3$, for formation of (a) *endo*-**7a** or *endo*-**7b** and (b) *exo*-**7a** or *exo*-**7b** from building blocks **2** and **3a**, and **2** and **3b**, respectively. Starting concentrations of diene and dienophile were 25 mM. ●: Reaction between **2** and **3b** (recognition-mediated reaction); ○: reaction between **2** and **3a** (bimolecular reaction); △: reaction between **2** and **3b** in the presence of 4 equiv of $PhCO_2H$ (competitive inhibitor); □: reaction between **2** and **3b** in the presence of preformed *endo*-**7b** (25 mol%) or *exo*-**7b** (7 mol%). Solid lines represent the best fit of experimental data to the appropriate kinetic model by using the SimFit[22] package. See Supporting Information for further details of the kinetic models used.

plex [**2**·**3b**] instead of the autocatalytic channel. The *endo*-selective binary-complex reactivity present within the complex [**2**·**3b**] was confirmed by kinetic simulation and fitting (Figure 5).

Single crystals,[24] suitable for X-ray diffraction, of *endo*-**7b** were grown by slow evaporation of a $CDCl_3$ solution of the cycloadduct. Surprisingly, *endo*-**7b** exists (Figure 6) in the solid state as a hydrogen-bonded homodimer. The presence of this duplex in the solid state suggests that *endo*-**7b** might be formed by replication. However, the kinetic data are completely consistent with reaction through the binary reactive complex [**2**·**3b**]. In particular, there is no evidence in the kinetic data that *endo*-**7b** is capable of templating its own formation, even if the reaction mixture is doped with relatively high levels (0.25 equiv) of *endo*-**7b**.

Therefore, we discount the observation of an *endo*-**7b** duplex in the solid state as simply an anomaly resulting from the crystallisation process. To satisfy ourselves that the complex [**2**·**3b**] was capable of accessing the transition state leading to *endo*-**7b**, we undertook a series of computational studies. Monte Carlo conformational searches performed by using the AMBER* forcefield[25] and the GB/SA solvation model for chloroform reveal that the lowest-energy conformations (Figure 7a) of *endo*-**7b** adopt a closed geometry with two hydrogen bonds under 2.00 Å in length. Ab initio electronic structure calculations performed at the B3LYP/6–31G(d)) level of theory by using the PCM solvation model[26] for chloroform reveal that a plausible transition

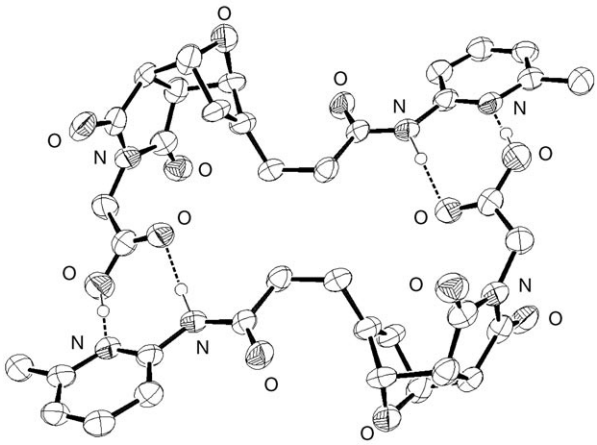

Figure 6. Ball-and-stick representation of the structure of cycloadduct *endo*-**7b** in the solid state determined by single-crystal X-ray diffraction.[24] The cycloadduct crystallises as a hydrogen-bonded duplex. Hydrogen atoms are omitted for clarity, except for those involved in hydrogen bonds. Hydrogen bonds are shown by dashed lines.

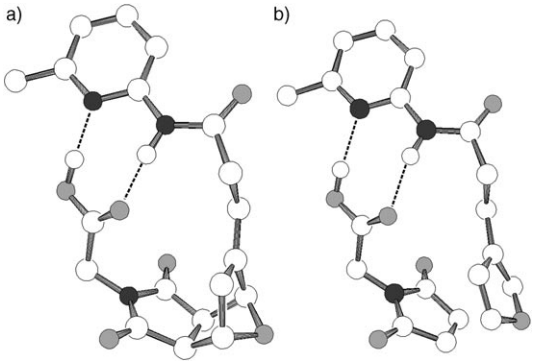

Figure 7. a) Ball-and-stick model of a representative low-energy conformation of *endo*-**7b** calculated by using the AMBER* forcefield. b) Ball-and-stick representation of the calculated (B3LYP/6–31G(d)) transition state for formation *endo*-**7b** within the [**2**·**3b**] complex. Carbon atoms white, oxygen atoms light grey, nitrogen atoms dark grey. Some hydrogen atoms are omitted for clarity. Hydrogen bonds are represented by dashed lines.

state for *endo*-**7b** can be accessed (Figure 7b) from the [**2**·**3b**] complex.

System 4: Analysis of the kinetic data (Figure 8) acquired for the reaction of diene **2** with dienophile **4a** revealed that the bimolecular reaction was rather unselective; [*endo*-**8a**]:[*exo*-**8a**] = 2:3. The introduction of recognition sites into the diene and dienophile resulted in a significant rate enhancement in the formation of *endo*-**8b**, and a smaller rate enhancement in the formation of *exo*-**8b**. This difference in rate acceleration between the diasteroisomers gives rise to a [*endo*-**8b**]:[*exo*-**8b**] ratio of 3:2 for the recognition-mediated reaction between **2** and **4b**. Kinetic analysis reveals that, although there is significant recognition-mediated acceleration of the formation of *endo*-**8b**, this acceleration occurs through the intermediacy of a binary complex rather than through autocatalysis. In the case of *exo*-**8b**, the recognition-mediated acceleration is rather smaller and its origins are difficult to define precisely. The lower degree of rate acceleration relative to either System 2 or System 3 is easily rationalised in terms of the additional CH_2 rotor that is present in System 4. The restriction of this rotor in the transition state leading to *endo*-**8b** will result in reaction via this species being disfavoured[27] by 10–15 eu relative to the corresponding transition-state structure for either *endo*-**6b** or *endo*-**7b**. Surprisingly, the addition of benzoic acid resulted in a small increase in the observed rate of reaction for *exo*-**8b**, despite showing the expected inhibitory effect in the production of *endo*-**8b**. Although reproducible, the origin of this effect is unclear.

Once again, it was possible to grow single crystals of *endo*-**8b** suitable for analysis[28] by X-ray diffraction. The cycloadduct crystallises (Figure 9) as a helical hydrogen-bonded polymer in which the carboxylic acid of one cycloadduct is hydrogen bonded to the amidopyridine ring of the adjacent cycloadduct along the crystallographic *b* direction. This dimeric subunit is then propagated through the structure by translation. The solid-state structure of *endo*-**8b** is

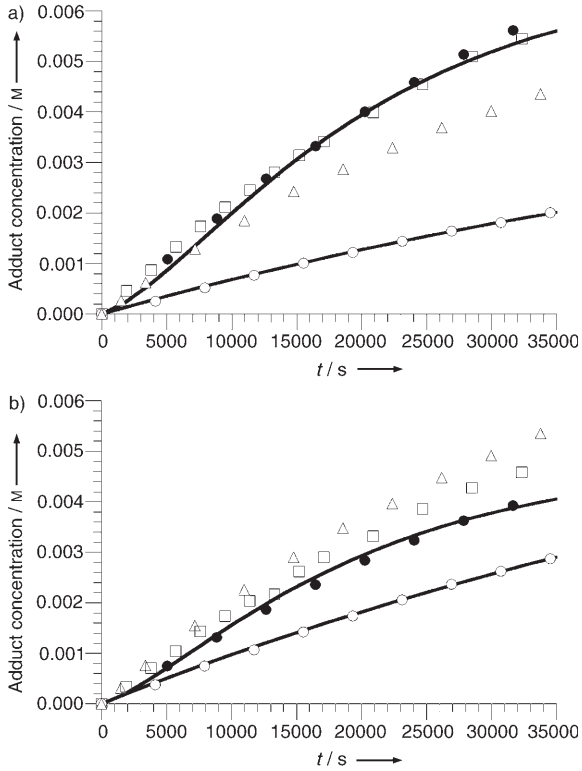

Figure 8. Rate profiles, at 308 K in $CDCl_3$, for formation of (a) *endo*-**8a** or *endo*-**8b** and (b) *exo*-**8a** or *exo*-**8b** from building blocks **2** and **4a**, and **2** and **4b**, respectively. Starting concentrations of diene and dienophile were 25 mM. ●: Reaction between **2** and **4b** (recognition-mediated reaction); ○: reaction between **2** and **4a** (bimolecular reaction); △: reaction between **2** and **4b** in the presence of 4 equiv of $PhCO_2H$ (competitive inhibitor); □: reaction between **2** and **4b** in the presence of preformed *endo*-**8b** (16 mol%) or *exo*-**8b** (13 mol%). Solid lines represent the best fit of experimental data to the appropriate kinetic model by using the SimFit[22] package. See Supporting Information for further details of the kinetic models used.

different to the calculated structure for the isolated molecule in solution. Conformational searches (AMBER*/GB/SA $CHCl_3$) identified a closed-template structure containing two hydrogen bonds as the minimum-energy conformation of *endo*-**8b**. This closed geometry is consistent with the formation of *endo*-**8b** through a binary reactive complex.

Given the wealth of experimental data acquired for Systems 1–4, some means of assessing global patterns of reactivity are required. Therefore, we calculated the relative rate enhancements for each diasteroisomer in Systems 1–4. The relative rate enhancement (RRE) for *each* diastereoisomer is the ratio of the recognition-mediated rate to the bimolecular rate. Therefore, a value of RRE greater than one indicates that the recognition-mediated reaction is faster than the bimolecular reaction for that diastereoisomer. Notably, within each system the *endo*:*exo* ratio is *not* represented by the ratio of RREs for the two diastereoisomers (Figure 10a). We also probed the changes in diastereoselectivity of the cycloaddition reactions by calculating the logarithm of the relative diastereoisomeric ratio, d.r. (Figure 10b). This measure is derived by taking the $\log_{10}$ of the ratio of the d.r. observed

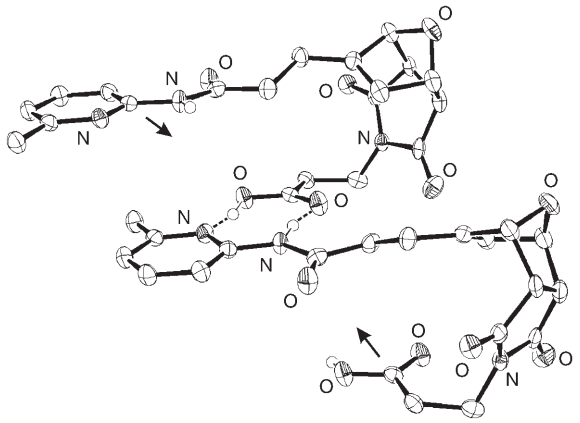

Figure 9. Ball-and-stick representation of the structure of cycloadduct *endo*-**8b** in the solid state determined[28] by single-crystal X-ray diffraction. The cycloadduct crystallises as a helical hydrogen-bonded polymer in which the carboxylic acid of one cycloadduct is hydrogen bonded to the amidopyridine ring of the adjacent cycloadduct along the crystallographic *b* axis. The direction of propagation of the helix is shown by the arrows. Hydrogen atoms are omitted for clarity, except for those involved in hydrogen bonds. Hydrogen bonds are represented by dashed lines. Arrows indicate the direction of hydrogen bonding to the adjacent dimer in the solid state. The dimers are related by translation along the crystallographic *b* direction.

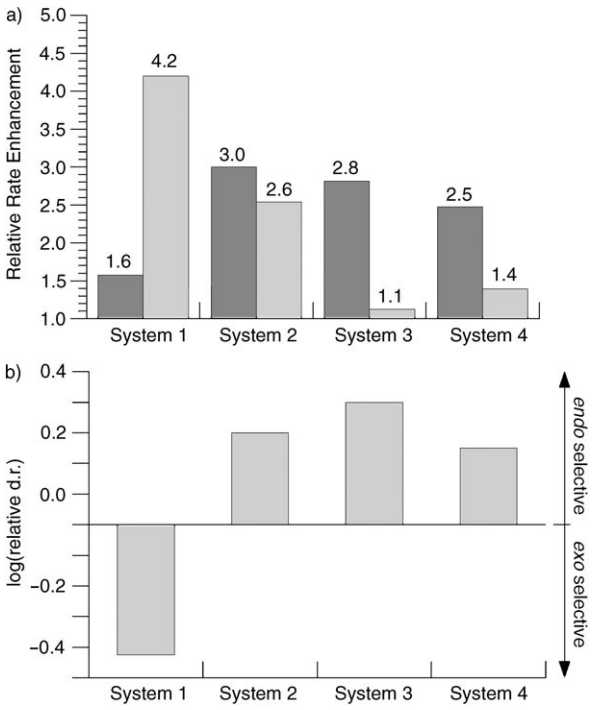

Figure 10. a) Comparison of the relative rate enhancements (RRE) observed for the *endo* (dark gray bars) and *exo* (light gray bars) diastereoisomers present in Systems 1–4. The RRE for each diastereoisomer is the ratio of the recognition-mediated rate to the bimolecular rate. RRE >1 indicates that the recognition-mediated reaction is faster than the bimolecular reaction. Note: within each system the *endo*:*exo* ratio is *not* represented by the relative heights of the bars. The RRE value is given above each bar. b) Comparison of log(relative d.r.) observed for each system. Log(relative d.r.) <0 indicates that the recognition-mediated reaction is more *exo* selective than the bimolecular reaction. Log(relative d.r.) >0 indicates that the recognition-mediated reaction is more *endo* selective than the bimolecular reaction.

for the recognition-mediated process to that observed for the control reaction. A log(relative d.r.) value of greater than zero indicates that the reaction becomes more *endo* selective if it is recognition-mediated, whereas a log(relative d.r.) value of less than zero indicates that the reaction becomes more *exo* selective if it is recognition-mediated.

In general, the bimolecular reaction shows little selectivity, with any slight preference being for the *endo* diastereoisomer. System 1 achieves a significant reversal of this diastereoselectivity by enhancing the formation of the *exo* diastereoisomer by a factor of four through autocatalysis. All of the other three systems become moderately more *endo* selective by enhancing the formation of the *endo* isomer by reaction within a favourable binary complex. The most-efficient system in terms of selectivity is System 3, which, although accelerating the formation of the *endo* diastereoisomer slightly less than System 2, is most selective by virtue of avoiding simultaneous acceleration of the corresponding *exo* diastereoisomer. This result is surprising as System 2 and System 3 have identical total numbers of CH_2 spacer units present within their overall structure; only the relative placement of these spacers is different.

Comparisons with a second series of structurally related systems described[29] previously (Systems 5–8, Scheme 3) are also instructive. In these systems, the orientation and reactivity of the diene component was altered by placing the tether connecting the diene to the recognition site at the 2-position of the furan ring as opposed to the 3-position described in this work.

By using previously published[29] experimental data acquired for Systems 5–8, we calculated the relative rate enhancements for each diastereoisomer in these systems as discussed above. The data are shown in Figure 11a. Once again, we probed the changes in diastereoselectivity of the cycloaddition reactions by calculating log(relative d.r.) (Figure 11b).

In general, the bimolecular reaction shows little selectivity (see Table S1, Supporting Information). However, in the case of 2-substituted furans, any slight preference for the *exo* diastereoisomer is based on steric effects associated with the ring substituent. Once again, the system with the shortest spacers, System 5, achieves a significant reversal of this diastereoselectivity by enhancing the formation of the *endo* diastereoisomer by a factor of almost four through autocatalysis. Two of the other three systems become moderately more *exo* selective by enhancing the formation of the *exo* isomer by reaction within a favourable binary complex. The most efficient system in terms of selectivity is System 6, which enhances the formation[30] of the *exo* diastereoisomer almost 20-fold and slows down the formation of the *endo* diastereoisomer five-fold. Once again the most efficient system operates through a binary complex and has three methylenes; one in the diene and two in the dienophile.

This superficial similarity, in terms of tether length, with System 3 hides a more subtle effect; the true origin of the rate acceleration and, hence, the observed selectivity. Two possible mechanisms could give rise to the observed selec-

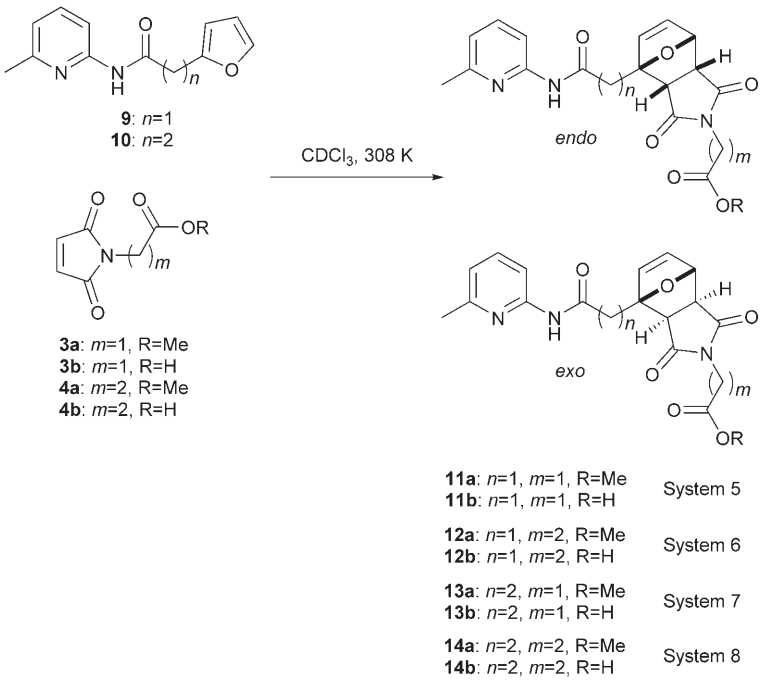

Scheme 3.

tivities. The first mechanism is selective stabilisation of the transition state leading to the *exo* (or *endo*) product over that leading to its diastereoisomer. The second mechanism is selective stabilisation of the *exo* (or *endo*) product itself over its diastereoisomer. The first of these mechanisms relies on a kinetic or transition-state effect, the second on a thermodynamic or ground-state effect. Fortunately, given our extensive kinetic data, we can probe which of these two effects are operating in System 3 and System 6. Calculation[31] of kinetic Effective Molarity[32] (kEM) and thermodynamic Effective Molarity[33] (tEM) is relatively straightforward. From our data, we find that the reactive binary complex responsible for the formation of *endo*-**7b** (System 3) generates a kEM of 0.22 M and a tEM of 1.57 M. This result suggests that ground-state stabilisation of *endo*-**7b** through the two hydrogen bonds present (Figure 12a) in the product is responsible for the observed *endo* selectivity. The kEM value suggests that although the transition state leading to *endo*-**7b** is stabilised with respect to the bimolecular process, this stabilisation

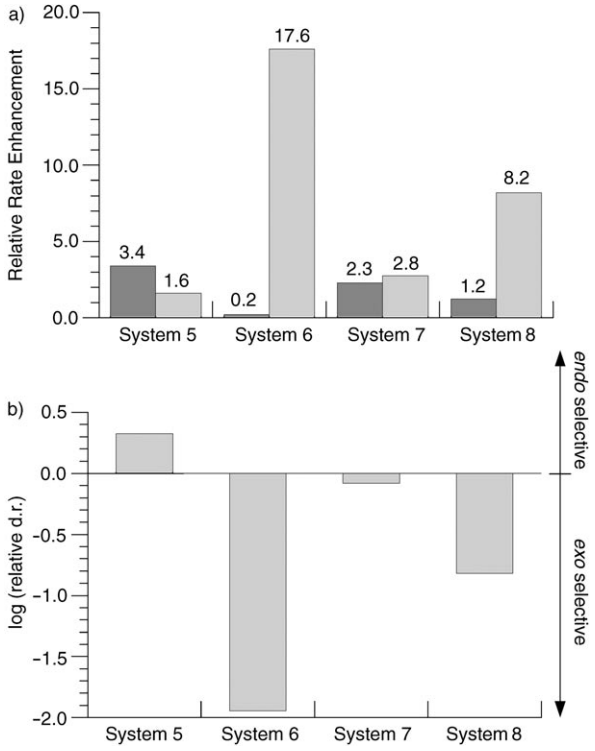

Figure 11. a) Comparison of the relative rate enhancements observed for the *endo* (dark gray bars) and *exo* (light gray bars) diastereoisomers present in Systems 5–8. The RRE value is given above each bar. b) Comparison of log(relative d.r.) observed for each system. Explicit definitions of RRE and log(relative d.r.) are provided in Figure 10.

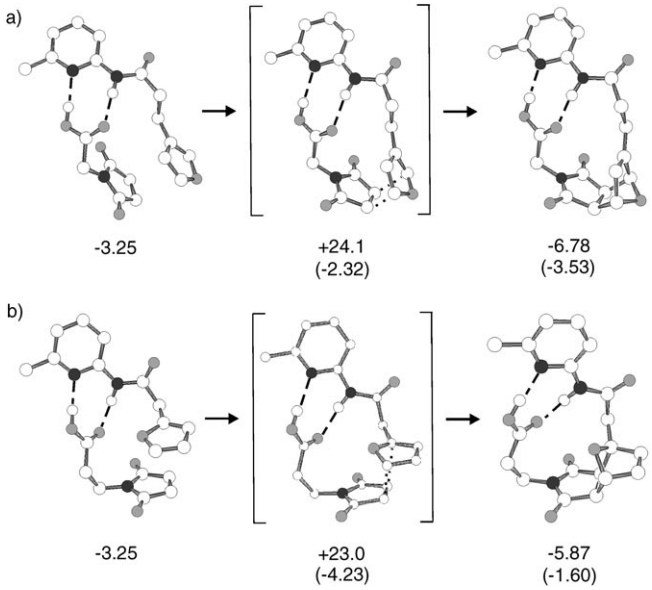

Figure 12. Selectivity is generated at different points on the pathways leading to (a) *endo*-**7b** and (b) *exo*-**12b**. All structures were calculated in the gas phase at the B3LYP/6–31G(d) level of theory. Energies are given relative to the arbitrary zero point of unbound diene and dienophile and are calculated from experimental data. Carbon atoms white, oxygen atoms light grey, nitrogen atoms dark grey. Some hydrogen atoms are omitted for clarity. Hydrogen bonds are represented by dashed lines. Energy values in brackets quantify the stabilisation of the transition state or ground state with respect to the same point on the reaction coordinate for the corresponding bimolecular reaction. All energies are in kcal.

(−2.32 kcal) is less than the binding energy of the binary complex and, hence, the kEM is less than 1 M. Therefore, stabilisation of the *endo*-**7b** ground state is the dominant effect. In contrast, the reactive binary complex responsible for the formation of *exo*-**12b** (System 6) generates a kEM of 2.60 M, whereas the tEM for the formation of *exo*-**12b** is only 68 mM. This result suggests that stabilisation (−4.23 kcal) of the transition state (Figure 12b) leading to *exo*-**12b**, which is accessed by the reactive binary complex [**9**·**4b**], is responsible for the observed selectivity.

Conclusion

We have elucidated the basic physical organic chemistry operating in a series of recognition-mediated cycloadditions. Within the four systems described here it is clear that, given sufficient conformational freedom, the most likely recognition-mediated pathway for reaction is that involving the binary complex (Channel 2, Figure 1). To generate autocatalytic systems, our original goal, we must ensure that this undesirable pathway is shut down. This can only be accomplished by using the shortest-possible tether length; one methylene group on the diene and one methylene group on the dienophile. Introduction of even a single additional methylene group beyond this minimum number effectively destroys reaction through the autocatalytic pathway (Channel 3, Figure 1). Therefore, an important lesson from this work is that design of efficient replicating systems almost certainly requires the selection of rigid spacers of mismatched length on the two building blocks, which provide the correct spatial orientation of the recognition sites whilst being compatible with the stereoelectronic demands of the cycloaddition reaction. Therefore, the design of the systems discussed here are less than optimal in that restriction of the spacers to various numbers of methylene groups provides too much conformational flexibility.

If the conformational freedom is restricted (e.g., System 1), the template is forced to adopt an open conformation. Replication is then possible, although weak in these systems. Although this conclusion is expected on the basis of entropic considerations, the different role of recognition in apparently similar systems (*endo*-**7b** versus *exo*-**12b**) is much more difficult to predict. The design and implementation of efficient and selective replication processes in structurally simple chemical systems remains an important and challenging goal.

Experimental Section

General procedures: All commercially available substrates, reagents and solvents were used without further purification. ^{1}H NMR spectra were recorded at 500.1 MHz by using either a Varian UNITYplus spectrometer or a Bruker Avance 500 spectrometer. ^{13}C NMR spectra were recorded at 125.6 MHz by using a Bruker Avance 500 spectrometer. Coupling constants (J) are given in Hz. High-resolution mass spectra were recorded by using either electron impact ionisation (EI) with a VG Autospec instrument or by using electrospray ionisation (ES) with a Micromass LCT spectrometer operating in negative-ion mode by the Mass Spectrometry Service at the University of St Andrews. Melting points were recorded by using an Electrothermal 9200 melting-point apparatus and are uncorrected.

Computational methods: Molecular mechanics calculations were carried out by using the AMBER* forcefield as implemented in Macromodel (Version 7.1, Schrödinger, **2000**) running on a Linux workstation. Ab initio electronic structure calculations were carried out by using GAMESS[34] running on a Linux cluster. The version dated 22 Nov 2004 was used in all calculations. The transition state for the reaction between furan and maleimide was located by generation of an initial guess by using the linear synchronous transit (LST) method and then refinement at the HF/6–31G(d) level of theory within GAMESS. This model transition state was then used to construct an initial guess for the transition state leading to the appropriate cycloadduct. This guess was refined at the B3LYP/6–31G(d) level of theory to a transition-state structure possessing single imaginary vibration that corresponded to the reaction coordinate.

Kinetic measurements: Reactions to acquire kinetic data were performed on an NMR scale. All stock solutions were prepared by dissolving the appropriate amount of a given reagent in the appropriate deuterated solvent by using a 2-cm^3 (2 cm^3 ± 0.02 mL accuracy) volumetric flask. Subsequent experimental samples were obtained by mixing a fixed amount of appropriate stock solutions by using Hamilton gas-tight syringes in a Wilmad 507PP or 528PP NMR tube, which was then fitted with a polyethylene pressure cap to minimise solvent evaporation. All stock solutions were pre-equilibrated at the appropriate reaction temperature for 1 h prior to mixing. After mixing, the sample was analysed by 500 MHz ^{1}H NMR spectrometry every 30 min by using either a Bruker Avance or a Varian UNITYplus 500 MHz NMR spectrometer. Spectra were analysed by using the deconvolution tool available within one-dimensional WINNMR. The errors in determination of the concentration of product, either by deconvolution of the analytical data or by experimental manipulation upon preparing the solution for analysis, are estimated to be ±4%. Kinetic simulation and fitting of the results data to the appropriate kinetic models was achieved by using SimFit. In all cases, the RMS error in the fit of the model to the experimental data was <3%.

2-Furan-3-yl-*N*-(6-methylpyridin-2-yl)-acetamide (1): The title compound was obtained as a colourless solid from furan-3-yl-acetic acid, in 53% yield, after column chromatography on SiO_2 (EtOAc/hexane, 2:5), by using a procedure reported[29] previously. M.p. 79.9–80.3 °C; ^{1}H NMR ($CDCl_3$, 300 MHz): δ = 8.01 (d, J = 8.19 Hz, 1H), 7.86 (br s, 1H), 7.58 (t, J = 7.81 Hz, 1H), 7.46 (d, J = 1.40 Hz, 2H), 6.89 (d, J = 7.56 Hz, 1H), 6.42 (t, J = 1.28 Hz, 1H), 3.57 (s, 2H), 2.42 ppm (s, 3H); ^{13}C NMR ($CDCl_3$, 125 MHz): δ = 168.8, 156.8, 150.35, 143.9, 140.95, 138.55, 119.4, 117.5, 111.2, 110.7, 34.2, 23.9 ppm; IR (KBr): $\tilde{\nu}$ = 3241, 3049, 1966, 1659, 1538, 1452, 1312, 1229, 1159, 1130, 1058, 1019, 793, 726 cm^{-1}; MS (EI+): m/z (%): 216 (100) $[M]^+$; HRMS (EI+): calcd for $C_{12}H_{12}N_2O_2$ $[M]^+$: 216.0899; found: 216.0900.

3-Furan-3-yl-*N*-(6-methylpyridin-2-yl)-propionamide (2): According to the procedure described[29] previously, the title compound was obtained from 3-furyl-propionic acid, in 60% yield, after column chromatography on SiO_2 (EtOAc/hexane, 2:5) as a colourless solid. M.p. 68.9–69.7 °C; ^{1}H NMR ($CDCl_3$, 300 MHz): δ = 8.00 (d, J = 8.20 Hz, 1H), 7.94 (br s, 1H), 7.59 (t, J = 7.80 Hz, 1H), 7.34 (t, J = 1.67 Hz, 1H), 7.27–7.255 (m, 1H), 6.89 (d, J = 7.43 Hz, 1H), 6.29–6.275 (m, 1H), 2.86 (t, J = 7.42 Hz, 2H), 2.60 (t, J = 7.42 Hz, 2H), 2.43 ppm (s, 3H); ^{13}C NMR ($CDCl_3$, 125 MHz): δ = 170.65, 156.5, 150.6, 142.8, 138.9, 138.5, 123.3, 119.1, 111.0, 110.6, 37.8, 23.7, 20.3 ppm; IR (KBr): $\tilde{\nu}$ = 3267, 2921, 1672, 1599, 1580, 1542, 1450, 1397, 1296, 1229, 1152, 1022, 965, 873, 782 cm^{-1}; MS (EI+): m/z (%): 230 (100) $[M]^+$; HRMS (EI+): calcd for $C_{13}H_{14}N_2O_2$ $[M]^+$: 230.1055; found: 230.1054.

***Endo*-{8-[(6-methylpyridin-2-ylcarbamoyl)-methyl]-3,5-dioxo-10-oxa-4-azatricyclo[5.2.1.0^{2,6}]dec-8-en-4-yl}acetic acid methyl ester (5a)**: The title compound was obtained as the major product after reacting together compounds **1** and **3a** in $CDCl_3$ followed by column chromatography on SiO_2 (EtOAc/hexane, 1:5) as a colourless oil. ^{1}H NMR ($CDCl_3$,

500 MHz): $\delta = 8.35$ (brs, 1H), 7.98 (d, $J = 8.11$ Hz, 1H), 7.57 (t, $J = 7.90$ Hz, 1H), 6.88 (d, $J = 7.47$ Hz, 1H), 6.27 (d, $J = 1.50$ Hz, 1H), 5.34 (d, $J = 4.70$ Hz, 1H), 5.31 (d, $J = 4.70$ Hz, 1H), 4.13 (q, $J = 17.08$ Hz, 2H), 3.80 (s, 3H), 3.66 (m, 2H), 3.37 (dd, $J = 16.65$ Hz, 1H), 3.21 (dd, $J = 1.07$, 16.87 Hz, 1H), 2.41 ppm (s, 3H); ^{13}C NMR ($CDCl_3$, 125 MHz): δ(*exo* only) = 175.9, 175.1, 170.0, 167.0, 156.6, 150.7, 150.4, 139.1, 129.4, 119.4, 111.0, 83.4, 81.9, 49.6, 47.2, 39.2, 35.3, 34.1, 22.3 ppm; MS (ES+): *m/z* (%): 386 (100) $[M+H]^+$; HRMS (ES+): calcd for $C_{19}H_{19}N_3O_6$ $[M+H]^+$: 386.1352; found: 386.1365.

{8-[(6-Methylpyridin-2-ylcarbamoyl)-methyl]-3,5-dioxo-10-oxa-4-azatricyclo[5.2.1.0^{2,6}]dec-8-en-4-yl}acetic acid (5b): The title compound, a colourless solid, was obtained as the major product after reacting together compounds **1** and **3b** in $CDCl_3$ and isolation of the product by using the method described[29] previously. M.p. 251.5–252.2 °C; ^{1}H NMR ([D$_6$]DMSO, 500 MHz): $\delta = 10.53$ (brs, 1H$_{endo}$), 10.51 (brs, 1H$_{exo}$), 7.96 (d, $J = 8.21$ Hz, 1H$_{endo}$), 7.86 (d, $J = 8.21$ Hz, 1H$_{exo}$), 7.65 (t, $J = 7.75$ Hz, 1H$_{endo}$), 7.64 (t, $J = 7.75$ Hz, 1H$_{exo}$), 6.95 (d, $J = 7.30$ Hz, 1H$_{endo}$, 1H$_{exo}$), 6.41 (brs, 1H$_{endo}$), 6.30 (d, $J = 1.36$ Hz, 1H$_{exo}$), 5.14 (brs, 1H$_{endo}$), 5.10 (brs, 1H$_{exo}$), 5.09 (brs, 1H$_{exo}$), 4.92 (d, $J = 5.17$ Hz, 1H$_{endo}$), 4.08 (s, 2H$_{endo}$), 4.05 (s, 2H$_{exo}$), 3.49–2.53 (m, 4H$_{endo}$, 4H$_{exo}$), 2.40 ppm (s, 3H$_{endo}$, 3H$_{exo}$); ^{13}C NMR ($CDCl_3$, 125 MHz): δ(*exo* only) = 176.8, 176.2, 171.0, 169.5, 154.2, 150.3, 144.7, 138.5, 132.2, 118.3, 110.6, 82.1, 81.1, 48.6, 47.1, 34.7, 30.6, 23.4 ppm; IR (KBr): $\tilde{\nu} = 3454$, 3002, 2368, 1775, 1708, 1660, 1592, 1453, 1424, 1381, 1328, 1265, 1179 cm^{-1}; MS (ES−): *m/z* (%): 370 (100) $[M-H]^+$; HRMS (ES−): calcd for $C_{18}H_{17}N_3O_6$ $[M-H]^+$: 370.1039; found: 370.1027.

3-{8-[(6-Methylpyridin-2-ylcarbamoyl)-methyl]-3,5-dioxo-10-oxa-4-azatricyclo[5.2.1.0^{2,6}]dec-8-en-4-yl}propionic acid (6b): The title compound was obtained as the major product after reacting together compounds **1** and **4b** in $CDCl_3$ followed by purification as described for compound **5b** to afford a colourless solid. M.p. 245.2–246.2 °C; ^{1}H NMR ([D$_6$]DMSO, 500 MHz): $\delta = 10.52$ (brs, 1H$_{endo}$), 10.50 (brs, 1H$_{exo}$), 7.94 (d, $J = 8.24$ Hz, 1H$_{endo}$), 7.85 (d, $J = 8.24$ Hz, 1H$_{exo}$), 7.64 (t, $J = 8.06$ Hz, 1H$_{exo}$), 7.63 (t, $J = 8.06$ Hz, 1H$_{endo}$), 6.95 (d, $J = 7.51$ Hz, 1H$_{exo}$), 6.93 (d, $J = 7.51$ Hz, 1H$_{endo}$), 6.38 (m, 1H$_{endo}$), 6.27 (d, $J = 1.46$ Hz, 1H$_{exo}$), 5.08 (s, 1H$_{endo}$), 5.05 (brs, 1H$_{exo}$), 5.03 (s, 1H$_{exo}$), 4.87 (d, $J = 5.13$ Hz, 1H$_{endo}$), 3.61–2.72 (m, 8H$_{endo}$, 6H$_{exo}$), 3.11 (d, $J = 6.59$ Hz, 1H$_{exo}$), 2.95 (d, $J = 6.59$ Hz, 1H$_{exo}$), 2.41 (s, 3H$_{endo}$), 2.39 ppm (s, 3H$_{exo}$); ^{13}C NMR ([D$_6$]DMSO, 125 MHz): δ(*exo* only) = 176.2, 176.0, 171.6, 168.2, 156.4, 151.1, 144.8, 138.3, 132.0, 118.6, 110.3, 82.4, 81.0, 48.3, 46.7, 35.3, 33.9, 31.6, 23.4 ppm; IR (KBr): $\tilde{\nu} = 3454$, 3079, 2367, 1770, 1703, 1616, 1582, 1453, 1400, 1376, 1313, 1260, 1159 cm^{-1}; MS (ES−): *m/z* (%): 385 (100) $[M-H]^+$; HRMS (ES−) calcd for $C_{19}H_{19}N_3O_6$ $[M-H]^+$: 384.1196; found: 384.1200.

***Endo*-{8-[2-(6-methylpyridin-2-ylcarbamoyl)-ethyl]-3,5-dioxo-10-oxa-4-azatricyclo[5.2.1.0^{2,6}]dec-8-en-4-yl}acetic acid methyl ester (7a)**: The title compound was obtained as the major product after reacting together compounds **2** and **3a** in $CDCl_3$ followed by column chromatography on SiO_2 (EtOAc/hexane, 2:5) to afford a colourless oil. ^{1}H NMR ($CDCl_3$, 500 MHz): $\delta = 8.46$ (brs, 1H), 7.99 (d, $J = 8.33$ Hz, 1H), 7.58 (t, $J = 8.11$ Hz, 1H), 6.87 (d, $J = 7.47$ Hz, 1H), 6.02 (d, $J = 1.71$ Hz, 1H), 5.29 (d, $J = 3.41$ Hz, 1H), 5.14 (d, $J = 3.41$ Hz, 1H), 4.18 (d, $J = 17.29$ Hz, 1H), 4.09 (d, $J = 17.29$ Hz, 1H), 3.86 (s, 3H), 3.63 (m, 2H), 2.77–2.66 (m, 2H), 2.56–2.42 (m, 2H), 2.40 ppm (s, 3H).

***Exo*-{8-[2-(6-methylpyridin-2-ylcarbamoyl)-ethyl]-3,5-dioxo-10-oxa-4-azatricyclo[5.2.1.0^{2,6}]dec-8-en-4-yl}acetic acid methyl ester (7a)**: The title compound was obtained as the major product after reacting together compounds **2** and **3a** in $CDCl_3$ followed by column chromatography on SiO_2 (EtOAc/hexane, 2:5). ^{1}H NMR ($CDCl_3$, 500 MHz): $\delta = 8.47$ (brs, 1H), 7.98 (d, $J = 7.90$ Hz, 1H), 7.605 (t, $J = 8.11$ Hz, 1H), 6.90 (d, $J = 7.47$ Hz, 1H), 6.08 (d, $J = 1.71$ Hz, 1H), 5.22 (s, 1H), 5.10 (s, 1H), 4.22 (s, 2H), 3.745 (s, 3H), 3.08 (d, $J = 6.62$ Hz, 1H), 2.97 (d, $J = 6.41$ Hz, 1H), 2.67–2.57 (m, 4H), 2.44 ppm (s, 3H); ^{13}C NMR ($CDCl_3$, 125 MHz): $\delta =$ 175.4, 175.3, 169.8, 167.0, 156.6, 150.7, 150.4, 139.1, 129.0, 119.4, 110.9, 83.2, 81.8, 49.3, 47.3, 39.5, 34.5, 23.6, 22.3, 21.2 ppm; MS (ES+): *m/z* (%): 400 (100) $[M+H]^+$; HRMS (ES+) calcd for $C_{20}H_{21}N_3O_6$ $[M+H]^+$: 400.1509; found: 400.1512.

***Exo*-{8-[2-(6-methylpyridin-2-ylcarbamoyl)-ethyl]-3,5-dioxo-10-oxa-4-azatricyclo[5.2.1.0^{2,6}]dec-8-en-4-yl}acetic acid (7b)**: The title compound was obtained as the major product after reacting together compounds **2** and **3b** in $CDCl_3$ followed by purification as described for compound **5b** to afford a colourless solid. M.p. 232.5–233.1 °C; ^{1}H NMR ([D$_6$]DMSO, 500 MHz): $\delta = 10.35$ (brs, 1H), 7.86 (d, $J = 8.24$ Hz, 1H), 7.63 (t, $J = 8.10$ Hz, 1H), 6.93 (d, $J = 7.51$ Hz, 1H), 6.10 (d, $J = 1.45$ Hz, 1H), 5.07 (brs, 1H), 5.02 (s, 1H), 4.04 (s, 2H), 3.12 (d, $J = 6.50$ Hz, 1H), 3.01 (d, $J = 6.50$ Hz, 1H), 2.63–2.46 (m, 4H), 2.38 ppm (s, 3H); ^{13}C NMR ([D$_6$]DMSO, 125 MHz): $\delta = 175.6$, 175.5, 170.95, 167.8, 156.3, 151.3, 150.3, 138.25, 128.9, 118.3, 110.3, 82.2, 81.0, 48.8, 46.7, 38.8, 33.7, 23.4, 22.3 ppm; IR (KBr): $\tilde{\nu} = 3453$, 3001, 2741, 2366, 1769, 1707, 1611, 1452, 1413, 1389, 1332, 1264, 1183, 1149 cm^{-1}; MS (ES−): *m/z* (%): 385 (100) $[M-H]^+$; HRMS (ES−) calcd for $C_{19}H_{19}N_3O_6$ $[M-H]^+$: 384.1196; found: 384.1194.

***Endo*-3-{8-[2-(6-methylpyridin-2-ylcarbamoyl)-ethyl]-3,5-dioxo-10-oxa-4-azatricyclo[5.2.1.0^{2,6}]dec-8-en-4-yl}propionic acid methyl ester (8a)**: The title compound was obtained as the major product after reacting together compounds **2** and **4a** in $CDCl_3$ followed by column chromatography on SiO_2 (EtOAc/hexane, 2:5). ^{1}H NMR ($CDCl_3$, 500 MHz): $\delta = 7.96$ (d, $J = 8.12$ Hz, 1H), 7.92 (brs, 1H), 7.58 (t, $J = 7.90$ Hz, 1H), 6.89 (d, $J = 7.48$ Hz, 1H), 5.98 (d, $J = 1.07$ Hz, 1H), 5.24 (d, $J = 4.91$ Hz, 1H), 5.12 (d, $J = 5.12$ Hz, 1H), 3.73–3.61 (m, 2H), 3.69 (s, 3H), 3.58–3.53 (m, 2H), 2.61–2.45 (m, 6H), 2.44 ppm (s, 3H).

***Exo*-3-{8-[2-(6-methylpyridin-2-ylcarbamoyl)-ethyl]-3,5-dioxo-10-oxa-4-azatricyclo[5.2.1.0^{2,6}]dec-8-en-4-yl}propionic acid methyl ester (8a)**: The title compound was obtained as the major product after reacting together compounds **2** and **4a** in $CDCl_3$ followed by column chromatography on SiO_2 (EtOAc/hexane, 2:5) to afford a colourless oil. ^{1}H NMR ($CDCl_3$, 500 MHz): $\delta = 7.94$ (d, $J = 7.90$ Hz, 1H), 7.85 (brs, 1H), 7.59 (t, $J = 7.90$ Hz, 1H), 6.91 (d, $J = 7.47$ Hz, 1H), 6.06 (d, $J = 1.28$ Hz, 1H), 5.18 (brs, 1H), 5.06 (s, 1H), 3.77 (t, $J = 7.36$ Hz, 2H), 3.67 (s, 3H), 2.96 (d, $J = 6.40$ Hz, 1H), 2.87 (d, $J = 6.41$ Hz, 1H), 2.66–2.56 (m, 6H), 2.45 ppm (s, 3H); MS (ES+): *m/z* (%): 414 (100) $[M+H]^+$; HRMS (ES+) calcd for $C_{21}H_{23}N_3O_6$ $[M+H]^+$: 414.1665; found: 414.1668.

{8-[2-(6-Methylpyridin-2-ylcarbamoyl)-ethyl]-3,5-dioxo-10-oxa-4-azatricyclo[5.2.1.0^{2,6}]dec-8-en-4-yl}propionic acid (8b): The title compound was obtained as the major product after reacting together compounds **2** and **4b** in $CDCl_3$ followed by purification as described for compound **5b** to afford a colourless solid. M.p. 85.6–86.4 °C; ^{1}H NMR ($CDCl_3$, 500 MHz): $\delta = 11.16$ (brs, 1H$_{endo}$), 10.82 (brs, 1H$_{exo}$), 8.12 (d, $J = 8.54$ Hz, 1H$_{exo}$), 8.11 (d, $J = 8.11$ Hz, 1H$_{endo}$), 7.655 (t, $J = 7.90$ Hz, 1H$_{endo}$), 7.65 (t, $J = 7.90$ Hz, 1H$_{exo}$), 6.88 (d, $J = 7.69$ Hz, 1H$_{endo}$, 1H$_{exo}$), 6.13 (d, $J = 1.28$ Hz, 1H$_{exo}$), 6.08 (d, $J = 1.28$ Hz, 1H$_{endo}$), 5.27 (d, $J = 5.13$ Hz, 1H$_{endo}$), 5.15 (brs, 1H$_{exo}$), 5.14 (s, 1H$_{exo}$), 5.07 (d, $J = 5.55$ Hz, 1H$_{endo}$), 3.84 (t, $J = 7.26$ Hz, 2H$_{exo}$), 3.80–3.76 (m, 1H$_{endo}$), 3.64–3.57 (m, 1H$_{endo}$), 3.58 (d, $J = 8.11$ Hz, 1H$_{endo}$), 3.53 (dd, $J = 5.55$, 8.11 Hz, 1H$_{endo}$), 2.91 (d, $J = 6.41$ Hz, 1H$_{exo}$), 2.88 (d, $J = 6.41$ Hz, 1H$_{exo}$), 2.86–2.43 (m, 6H$_{endo}$, 6H$_{exo}$), 2.42 ppm (s, 3H$_{endo}$, 3H$_{exo}$); ^{13}C NMR ($CDCl_3$, 125 MHz, *endo* diastereoisomer in parentheses): $\delta = 176.8$, 176.6 (176.15), 176.0 (175.1) (174.3) (171.6), 171.2, 155.7 (155.5) (151.3), 151.1, 150.4 (149.9) (140.4), 140.3, 129.6 (125.6), 119.5 (119.3), 111.9 (111.9), 82.9 (82.3), 81.8 (80.3), 49.1, 47.2 (47.2) (47.0) (36.2), 34.9 (34.8), 34.75, 32.2 (31.55) (25.6), 23.1, 22.0 (22.0 ppm); IR (KBr): $\tilde{\nu} = 3453$, 3001, 2741, 2366, 1769, 1707, 1611, 1452, 1413, 1389, 1332, 1264, 1183, 1149 cm^{-1}; MS (ES−): *m/z* (%): 398 (100) $[M-H]^+$; HRMS (ES−) calcd for $C_{20}H_{21}N_3O_6$ $[M-H]^+$: 398.1352; found: 398.1357.

Acknowledgements

This work was supported by the BBSRC (Grant 6/11855), the EPSRC (DTA award to E.K.) and the University of St Andrews. We thank Carolyn Horsburgh and Melanja Smith for technical assistance with HRMS and NMR, respectively, and Prof. G. von Kiedrowski for providing us with a copy of his SimFit program.

[1] a) H. Oikawa, K. Katayama, Y. Suzuki, A. Ichihara, *J. Chem. Soc. Chem. Commun.* **1995**, 1321–1322; b) K. Auclair, A. Sutherland, J.

Kennedy, D. J. Witter, J. P. van der Heever, C. R. Hutchinson, J. C. Vederas, *J. Am. Chem. Soc.* **2000**, *122*, 11519–11520; c) K. Watanabe, T. Mie, A. Ichihara, H. Oikawa, M. Honma, *J. Biol. Chem.* **2000**, *275*, 38393–38401.

[2] L. R. Domingo, *Eur. J. Org. Chem.* **2004**, 4788–4793.

[3] a) W. G. Dauben, H. O. Krabbenhoft, *J. Am. Chem. Soc.* **1976**, *98*, 1992–1993; b) W. G. Dauben, C. R. Kessel, K. H. Takemura, *J. Am. Chem. Soc.* **1980**, *102*, 6893–6894.

[4] a) P. A. Grieco, M. D. Kaufman, J. F. Daeuble, N. Saito, *J. Am. Chem. Soc.* **1996**, *118*, 2095–2096; b) I. Hemeon, C. De Amicis, H. Jenkins, P. Scammells, R. D. Singer, *Synlett* **2002**, 1815–1818.

[5] A. Kumar, *Chem. Rev.* **2001**, *101*, 1–20.

[6] a) F. Brion, *Tetrahedron Lett.* **1982**, *23*, 5299–5302; b) D. A. Smith, *Tetrahedron Lett.* **1991**, *32*, 1549–1552; c) P. A. Grieco, S. T. Handy, J. P. Beck, *Tetrahedron Lett.* **1994**, *35*, 2663–2666; d) A. Guy, L. Serva, *Synlett* **1994**, 647–648; e) H. Bienayme, A. Longeau, *Tetrahedron* **1997**, *53*, 9637–9646; f) S. Sankararaman, J. E. Nesakumar, *Eur. J. Org. Chem.* **2000**, 2003–2011.

[7] T. Ose, K. Watanabe, T. Mie, M. Honma, H. Watanabe, M. Yao, H. Oikawa, I. Tanaka, *Nature* **2003**, *422*, 186–189.

[8] a) A. J. Kirby, *Angew. Chem.* **1996**, *108*, 770–790; *Angew. Chem. Int. Ed. Engl.* **1996**, *35*, 707–724; b) S. J. Rowan, J. K. M. Sanders, *Curr. Opin. Chem. Biol.* **1997**, *1* 483–490; c) C. J. Walter, H. L. Anderson, J. K. M. Sanders, *J. Chem. Soc. Chem. Commun.* **1993**, 458–460; d) C. J. Walter, J. K. M. Sanders, *Angew. Chem.* **1995**, *107*, 223–225; *Angew. Chem. Int. Ed. Engl.* **1995**, *34*, 217–219; e) I. Huc, R. J. Pieters, J. Rebek, Jr., *J. Am. Chem. Soc.* **1994**, *116*, 11592–11593; f) R. J. Pieters, I. Huc, J. Rebek, Jr., *Chem. Eur. J.* **1995**, *1*, 183–192; g) A. Mulder, J. Huskens, D. N. Reinhoudt, *Org. Biomol. Chem.* **2004**, *2*, 3409–3424; h) G. M. Whitesides, M. Boncheva, *Proc. Natl. Acad. Sci. USA* **2002**, *99*, 4769–4774; i) G. M. Whitesides, B. Grzybowski, *Science* **2002**, *295*, 2418–2421; j) H. Cölfen, S. Mann, *Angew. Chem.* **2003**, *115*, 2452–2468; *Angew. Chem. Int. Ed.* **2003**, *42*, 2350–2365; k) I. W. Hamley, *Angew. Chem.* **2003**, *115*, 1730–1752; *Angew. Chem. Int. Ed.* **2003**, *42*, 1692–1712; l) G. W. Gokel, W. M. Leevy, M. E. Weber, *Chem. Rev.* **2004**, *104*, 2723–2750, and references therein; m) J. W. Lee, S. Samal, N. Selvapalam, H.-J. Kim, K. Kim, *Acc. Chem. Res.* **2003**, *36*, 621–630, and references therein; n) F. W. B. van Leeuwen, H. Beijleveld, H. Kooijman, A. L. Spek, W. Veboom, D. N. Reinhoudt, *J. Org. Chem.* **2004**, *69*, 3928–3936, and references therein; o) R. Martínez-Mánez, F. Sancenón, *Chem. Rev.* **2003**, *103*, 4419–4476; p) P. D. Beer, P. A. Gale, *Angew. Chem.* **2001**, *113*, 502–532; *Angew. Chem. Int. Ed.* **2001**, *40*, 486–516; q) J. Rebek, Jr., *Angew. Chem.* **2005**, *117*, 2104–2115; *Angew. Chem. Int. Ed.* **2005**, *44*, 2068–2078.

[9] a) P. G. Schultz, *Angew. Chem.* **1989**, *101*, 1336–1348; *Angew. Chem. Int. Ed. Engl.* **1989**, *28*, 1283–1295; b) X. Zhang, Q. Deng, S. H. Yoo, K. N. Houk, *J. Org. Chem.* **2002**, *67*, 9043–9053.

[10] a) G. von Kiedrowski, *Angew. Chem.* **1986**, *98*, 932–934; *Angew. Chem. Int. Ed. Engl.* **1986**, *25*, 932–935; b) G. von Kiedrowski, B. Wlotzka, J. Helbing, M. Matzan, S. Jordan, *Angew. Chem.* **1991**, *103*, 456–459; *Angew. Chem. Int. Ed. Engl.* **1991**, *30*, 423–426.

[11] a) L. J. Prins, D. N. Reinhoudt,, P. Timmerman, *Angew. Chem.* **2001**, *113*, 2446–2492; *Angew. Chem. Int. Ed.* **2001**, *40*, 2382–2426; b) F. Diederich, P. J. Stang, *Templated Organic Synthesis*, Wiley-VCH, Weinheim, **2000**; c) D. Philp, J. F. Stoddart, *Angew. Chem.* **1996**, *108*, 1242–1286; *Angew. Chem. Int. Ed. Engl.* **1996**, *35*, 1154–1196; d) C. Niemeyer, *Angew. Chem.* **2001**, *113*, 4254–4287; *Angew. Chem. Int. Ed.* **2001**, *40*, 4128–4158; e) J.-M. Lehn, *Chem. Eur. J.* **2000**, *6*, 2097–2102; f) T. Steiner, *Angew. Chem.* **2002**, *114*, 50–80; *Angew. Chem. Int. Ed.* **2002**, *41*, 48–76; g) G. Cooke, V. M. Rotello, *Chem. Soc. Rev.* **2002**, *31*, 275–286; h) D. C. Sherrington, K. Taskinen, *Chem. Soc. Rev.* **2001**, *30*, 83–93.

[12] a) D. Philp, A. Robertson, *Chem. Commun.* **1998**, *879*–880; b) C. A. Booth, D. Philp, *Tetrahedron Lett.* **1998**, *39*, 6987–6990; c) A. Robertson, D. Philp, N. Spencer, *Tetrahedron* **1999**, *55*, 11365–11384; d) R. M. Bennes, B. M. Kariuki, K. D. M. Harris, D. Philp, N. Spencer, *Org. Lett.* **1999**, *1*, 1087–1090; e) R. M. Bennes, M. Sapro-Babiloni, W. C. Hayes, D. Philp, *Tetrahedron Lett.* **2001**, *42*, 2377–2380; f) S. J. Howell, D. Philp, N. Spencer, *Tetrahedron* **2001**, *57*, 4945–4954.

[13] a) W. Oppolzer, *Angew. Chem.* **1977**, *89*, 10–24; *Angew. Chem. Int. Ed. Engl.* **1977**, *16*, 10–23; b) G. Brieger, J. N. Bennett, *Chem. Rev.* **1980**, *80*, 63–97; c) D. Craig, *Chem. Soc. Rev.* **1987**, *16*, 187–238; d) S. C. Hirst, A. D. Hamilton, *J. Am. Chem. Soc.* **1991**, *113*, 382–383.

[14] a) K. Mikami, M. Yamanaka, *Chem. Rev.* **2003**, *103*, 3369–3400; b) M. H. Todd, *Chem. Soc. Rev.* **2002**, *31*, 211–222.

[15] For comprehensive kinetic analyses of minimal systems, see: a) G. von Kiedrowski, *Bioorganic Chemistry Frontiers, Vol. 3*, Springer-Verlag, Berlin, Heidelberg, **1993**, pp. 115–146; b) D. N. Reinhoudt, D. M. Rudkevich, F. de Jong, *J. Am. Chem. Soc.* **1996**, *118*, 6880–6889; c) F. M. Menger, A. V. Eliseev, N. A. Khanjin, M. J. Sherrod, *J. Org. Chem.* **1995**, *60*, 2870–2878.

[16] a) S. P. Mathew, H. Iwamura, D. G. Blackmond, *Angew. Chem.* **2004**, *116*, 3379–3383; *Angew. Chem. Int. Ed.* **2004**, *43*, 3317–3321; b) D. G. Blackmond, *Proc. Natl. Acad. Sci. USA* **2004**, *101*, 5732–5736; c) F. G. Buono, H. Iwamura, D. G. Blackmond, *Angew. Chem.* **2004**, *116*, 2151–2155; *Angew. Chem. Int. Ed.* **2004**, *43*, 2099–2103; d) K. Soai, T. Shibata, H. Morioka, K. Choji, *Nature* **1995**, *378*, 767–768; e) T. Shibata, K. Choji, T. Hayase, Y. Aizu, K. Soai, *Chem. Commun.* **1996**, 1235–1236; f) T. Shibata, H. Morioka, T. Hayase, K. Choji, K. Soai, *J. Am. Chem. Soc.* **1996**, *118*, 471–472.

[17] For replication of more complex entities, see: a) J. W. Szostak, D. P. Bartel, P. L. Luisi, *Nature* **2001**, *409*, 387–390; b) R. Wick, P. Walde, P. L. Luisi, *J. Am. Chem. Soc.* **1995**, *117*, 1435–1436; A. Veronese, P. L. Luisi, *J. Am. Chem. Soc.* **1998**, *120*, 2662–2663; c) G. Ashkenasy, R. Jegasia, M. Yadav, M. R. Ghadiri, *Proc. Natl. Acad. Sci. USA* **2004**, *101*, 10872–10877; d) G. Ashkenasy, M. R. Ghadiri, *J. Am. Chem. Soc.* **2004**, *126*, 11140–11141; e) V. Zykov, E. Mytilinaios, B. Adams, H. Lipson, *Nature* **2005**, *435*, 163–164.

[18] Previous efforts by other groups focused purely on rate acceleration of the binding event through hydrogen-bonding recognition. We opted for cycloaddtion reactions yielding diastereoisomeric products, because these provide simultaneously scope for selectivity investigations.

[19] a) J. D. Winkler, *Chem. Rev.* **1996**, *96*, 167–176; b) C. Cativiela, J. I. Garcia, J. A. Mayoral, L. Salvatella, *Chem. Soc. Rev.* **1996**, *25*, 209–218; c) H. B. Kagan, O. Riant, *Chem. Rev.* **1992**, *92*, 1007–1019.

[20] a) F. H. Allen, W. D. Samuel Motherwell, P. R. Raithby, G. P. Shields, R. Taylor, *New J. Chem.* **1999**, *23*, 25–34; b) J. Bernstein, R. E. Davis, L. Shimoni, N.-L. Chang, *Angew. Chem.* **1995**, *107*, 1689–1708; *Angew. Chem. Int. Ed. Engl.* **1995**, *34*, 1555–1573; c) M. C. Etter, *Acc. Chem. Res.* **1990**, *23*, 120–126; d) T. Steiner, *Acta Crystallogr. Sect. B* **2001**, *57*, 103–106; e) F. Garcia-Tellado, S. J. Geib, S. Goswami, A. D. Hamilton, *J. Am. Chem. Soc.* **1991**, *113*, 9265–9269; f) J. Geib, C. Vincent, E. Fan, A. D. Hamilton, *Angew. Chem.* **1993**, *105*, 83–85; *Angew. Chem. Int. Ed. Engl.* **1993**, *32*, 119–121; g) E. Fan, J. Yang, J. Geib, T. C. Stoner, M. D. Hopkins, A. D. Hamilton, *J. Chem. Soc. Chem. Commun.* **1995**, 1251–1252; h) B. König, O. Möller, P. Bubenitschek, *J. Org. Chem.* **1995**, *60*, 4291–4293; i) I. L. Karle, D. Ranganathan, V. Haridas, *J. Am. Chem. Soc.* **1997**, *119*, 2777–2783; j) C. Bielawski, Y.-S. Chen, P. Zhang, P.-J. Prest, J. S. Moore, *Chem. Commun.* **1998**, 1313–1314; k) N. Shan, A. D. Bond, W. Jones, *Tetrahedron Lett.* **2002**, *43*, 3101–3104.

[21] J. I. Garcia, J. A. Mayoral, L. Salvatella, *Eur. J. Org. Chem.* **2005**, 85–90.

[22] G. von Kiedrowski, SimFit, version 1.0, program for analysis of kinetic data, **1994**.

[23] E. Kassiandis, R. J. Pearson, D. Philp, *Org. Lett.* **2005**, *7*, 3833–3836.

[24] X-ray diffraction studies on crystals of *endo*-**7b** grown from deuterated chloroform were performed by using a Rigaku Rapid/MM007/Cu system. The structure was solved by direct methods, the non-hydrogen atoms were refined (ref. [35]) with anisotropic displacement parameters, hydrogen atoms bound to carbon were idealised and fixed (C–H = 0.95 Å). Crystal data for *endo*-**7b**; $C_{19}H_{19}N_3O_6$, colourless plate, $0.1\times0.03\times0.001$ mm, $M_r = 385.37$, triclinic, $a = 7.0368(5)$ $b = 9.7060(7)$ $c = 14.0319(8)$ Å, $\alpha = 108.544(4)$ $\beta = 97.167(5)$ $\gamma =$

103.401(5)°, $F(000)=404$, $V=863.16(10)$ Å^3, $T=293$ K, space group $P\bar{1}$, $Z=2$, μ ($Cu_{K\alpha}$) $=0.942$ mm^{-1}, $2\theta_{max}=139.34°$. Of 2825 measured data 1198 were unique reflections ($R_{int}=0.0402$) to give $R1$ [$I>2\sigma(I)$] $=0.0726$ and $wR2=0.1948$. CCDC 230705 contains the supplementary crystallographic data (excluding structure factors) for this paper. These data can be obtained free of charge from The Cambridge Crystallographic Data Centre via www.ccdc.cam.ac.uk/data request/cif.

[25] Macromodel, Version 7.1, Schrödinger, USA, **2000**.

[26] a) S. Miertus, E. Scrocco, J. Tomasi, *Chem. Phys.* **1981**, *55*, 117–129; b) J. Tomasi, M. Persico, *Chem. Rev.* **1994**, *94*, 2027–2094; c) R. Cammi, J. Tomasi, *J. Comput. Chem.* **1995**, *16*, 1449–1458; d) H. Li, C. S. Pomelli, J. H. Jensen, *Theor. Chem. Acc.* **2003**, *109*, 71–84; e) H. Li, J. H. Jensen, *J. Comput. Chem.* **2004**, *25*, 1449–1462.

[27] a) M. I. Page, W. P. Jencks, *Proc. Natl. Acad. Sci. USA* **1971**, *68*, 1678–1680; b) M. I. Page, *Philos. Trans. R. Soc. London Ser. B* **1991**, *332*, 149–153.

[28] X-ray diffraction studies on crystals of *endo*-**8b** grown from deuterated chloroform were performed by using a Bruker SMART $Mo_{K\alpha}$ diffractometer. The structure was solved by direct methods, the non-hydrogen atoms were refined (ref. [35]) with anisotropic displacement parameters, hydrogen atoms bound to carbon were idealised and fixed (C–H 0.95 Å). Crystal data for *endo*-**8b**; $C_{21}H_{21}Cl_3N_3O_6$, colourless prism, $0.15\times0.1\times0.02$ mm, $M_r=518.77$, monoclinic, $a=15.416(3)$ $b=117.931(4)$ $c=8.3896(18)$ Å, $\beta=94.035(4)°$, $F(000)=1072$, $V=2313.3(9)$ Å^3, $T=125$ K, space group $P2_1/c$, $Z=4$, μ ($Mo_{K\alpha}$) $=0.440$ mm^{-1}, $2\theta_{max}=46.92°$. Of 11289 measured data 3287 were unique reflections ($R_{int}=0.0896$) to give $R1$ [$I>2\sigma(I)$] $=0.0492$ and $wR2=0.0885$. CCDC 230706 contains the supplementary crystallographic data (excluding structure factors) for this paper. These data can be obtained free of charge from The Cambridge Crystallographic Data Centre via www.ccdc.cam.ac.uk/data request/cif.

[29] a) R. J. Pearson, E. Kassianidis, D. Philp, *Tetrahedron Lett.* **2004**, *45*, 4777–4780; b) R. J. Pearson, E. Kassianidis, A. M. Z. Slawin, D. Philp, *Org. Biomol. Chem.* **2004**, *2*, 3434–3441.

[30] In fact, System 6 is more selective than described here. The *endo* cycloadduct is undetectable by 500 MHz ^{1}H NMR spectroscopy in the recognition-mediated reaction mixture. To calculate the log(relative d.r.) value, we have assumed that the final concentration of the *endo* adduct is just below the limit of detection (about 50 μM). Therefore, the value for log(relative d.r.) given for System 6 almost certainly underestimates the diastereoselectivity of this system.

[31] a) A. J. Kirby, *Adv. Phys. Org. Chem.* **1980**, *17*, 183–278; b) L. Mandolini, *Adv. Phys. Org. Chem.* **1986**, ***22***, 1–111; c) R. Cacciapaglia, S. Di Stefano, L. Mandolini, *Acc. Chem. Res.* **2004**, *37*, 113–122.

[32] The kinetic effective molarity is defined as the rate constant for the intracomplex reaction divided by the rate constant for the corresponding bimolecular reaction.

[33] The equilibrium or thermodynamic effective molarity is defined as the equilibrium constant for the intracomplex reaction divided by the equilibrium constant for the corresponding bimolecular reaction. In practice, this can be derived from the kinetic data by expressing the equilibrium constant (K_{eq}) as a ratio of the rate constants for the appropriate forward and reverse processes ($k_{forward}/k_{reverse}$).

[34] M. W. Schmidt, K. K. Baldridge, J. A. Boatz, S. T. Elbert, M. S. Gordon, J. H. Jensen, S. Koseki, N. Matsunaga, K. A. Nguyen, S. J. Su, T. L. Windus, M. Dupuis, J. A. Montgomery, *J. Comput. Chem.* **1993**, *14*, 1347–1363.

[35] G. M. Sheldrick, SHELXTL, version 6.10, program for crystal structure solution, Bruker AXS, Madison, **2002**.

Received: September 27, 2005
Revised: March 8, 2006
Published online: June 6, 2006

